

# Non-Markovian Quantum Heat Statistics with the Reaction Coordinate Mapping

Mike Shubrook\*

*Quantum Engineering Centre for Doctoral Training,  
H. H. Wills Physics Laboratory and Department of Electrical and Electronic Engineering,  
University of Bristol, BS8 1FD, United Kingdom*

Jake Iles-Smith and Ahsan Nazir

*Department of Physics and Astronomy, University of Manchester,  
Oxford Road, Manchester M13 9PL, United Kingdom*

The definition of heat in quantum mechanics is ambiguous. Complications arise in particular when the coupling between a quantum system and an environment is non-negligible, as the boundary between the two becomes blurred, making the distinction between system and environment difficult to draw. The reaction coordinate mapping can be used in such regimes to redraw the boundary between the system and environment. Here we combine the reaction coordinate technique with a two-point measurement protocol to compare two different definitions of heat: energetic changes in the full environment Hamiltonian (prior to the mapping), and energetic changes in the residual environment Hamiltonian (after the mapping). We find that the latter definition displays behaviour more expected of a thermal environment in the highly non-Markovian regime considered.

## I. INTRODUCTION

In classical thermodynamics, a distinction is drawn between two classes of observable quantities: A *state function* is a physical quantity, such as temperature or internal energy, that is well defined for each point in the system's phase space. In contrast, a *path function* is a physical quantity that depends on the specific path taken between two points in this phase space, for example heat and work. In a quantum mechanical setting, state functions can generally be represented as the trace of some Hermitian operator with the state of the system, or deduced from the state itself. However, path functions, such as work, do not have a clear analogue [1]. Notably, this has generated significant debate within the quantum thermodynamics community regarding the appropriate definition of heat and work in quantum systems [2–10].

In regimes where system-environment interactions are weak, and are therefore accurately captured by a Born-Markov master equation, heat can quite naturally be identified as the energy irreversibly emitted into (or absorbed from) the environment [3]. However, when the interaction energy becomes comparable to the internal energy of the system, there is no longer a clear partition between system and environment degrees of freedom [11, 12] as the two become strongly correlated, potentially exchanging energy in a non-Markovian (or reversible) fashion. This leads to further ambiguity as to how one should appropriately apportion the internal and interaction energies into heat and work [3, 7, 9, 13, 14].

In this paper, we investigate the role that different system-environment partitions play on quantum heat statistics in the non-Markovian regime. To do so, we employ the reaction coordinate mapping (RCM) of the

spin-boson model [15]. Here a collective coordinate of the environment is incorporated into an enlarged effective system Hamiltonian (the 'extended system'), with the remaining environment degrees of freedom included as a *residual environment* which may be treated perturbatively using the reaction coordinate master equation (RCME). The resulting description has proven useful in studying the dynamics [16–18] and thermodynamics [19–22] of quantum systems in regimes of strong and non-Markovian system-environment interactions. We extend the reaction coordinate formalism to the two-point measurement protocol (TPMP) [2, 23, 24] for the spin-boson model to derive a *heat-counting reaction coordinate master equation* (HC-RCME). This generalised master equation then allows us to calculate the characteristic function that generates the stochastic heat probability distribution for strong system-environment interactions.

Central to this work are the two possible definitions of heat provided by the RC formalism. Heat may naturally be defined as changes in the Hamiltonian of the environment prior to the mapping (the 'full environment'), or changes in the Hamiltonian of the residual environment after the mapping. We find that the two possible definitions of heat demonstrate qualitative and quantitative differences in the first two moments of their probability distributions. We also find corresponding differences in the change in ergotropy [25, 26] of the original system and the extended system over the process considered.

The paper is outlined as follows. In Section II A we cover the TPMP, outlining how the characteristic function of heat transfer can be written as the trace of a generalised density operator. In Section II B we show how the RCM can be used in conjunction with the TPMP to probe quantum heat statistics in the strong coupling regime, by deriving an equation of motion for the generalised density operator, and also introduce the two possible definitions of heat stated above. In Section III A we plot the characteristic functions of the two definitions

---

\* mikejshubrook@gmail.com

of heat, before looking at the first two moments of the corresponding probability distributions in Section III B. Differences in the first moment of these two definitions of heat motivates looking into the transfer of ordered energy (ergotropy), which we cover in Section III C. We summarise and conclude in Section IV.

## II. COUNTING STATISTICS IN THE STRONG COUPLING REGIME

Path functions do not have a clear and unambiguous definition in quantum systems; notably there are no unique Hermitian operators, and thus observables, associated to them. In order to define the statistics of path functions we consider performing projective measurements. The two-point measurement protocol [2, 3, 5] is a framework which can be used to calculate the full counting statistics of the path function we want to define. However, within the TPMP there is ambiguity in choosing what basis we perform these projective measurements onto. In the strong coupling and non-Markovian regime that we consider, choosing a particular basis to perform the projective measurements onto is not always straightforward.

### A. The two-point measurement protocol

We define changes in heat through the TPMP, a brief overview of which can be seen schematically in Fig. 1 and is as follows: An open quantum system  $S$  is coupled to an environment  $E$ , which together are governed by the Hamiltonian  $\hat{H}$ , evolving unitarily according to  $\hat{U}(t) = \exp[-i\hat{H}t]$ . To find the heat transfer within the composite system (system-plus-environment) we first prepare a product state  $\hat{\rho}(0) = \hat{\rho}_S(0) \otimes \hat{\rho}_E^{\text{th}}$ , where  $\hat{\rho}_E^{\text{th}}$  is a Gibbs state of the environment and  $\hat{\rho}_S(0)$  is an arbitrary initial state of the system. Next, a projective measurement of an observable  $\hat{M}$  is applied to the composite system, which is then allowed to evolve unitarily before performing a second projective measurement of  $\hat{M}$ . We define the difference of these two measurement outcomes as  $M$ , a stochastic quantity. By repeating the protocol many times we build up a probability distribution  $P(M, t)$ , where  $t$  is the time after the first measurement that we perform the second measurement. Our choice of operator  $\hat{M}$  leads to the definition of heat that we use.

While the probability distribution  $P(M, t)$  contains the statistics that we are interested in, it is more convenient to work with its Fourier transform, the characteristic function (CF),

$$\Phi(\chi, t) = \frac{1}{2\pi} \int_{-\infty}^{\infty} dM P(M, t) e^{iM\chi}, \quad (1)$$

a complex valued function of the *counting parameter*  $\chi$ , which is the conjugate parameter to the stochastic quan-

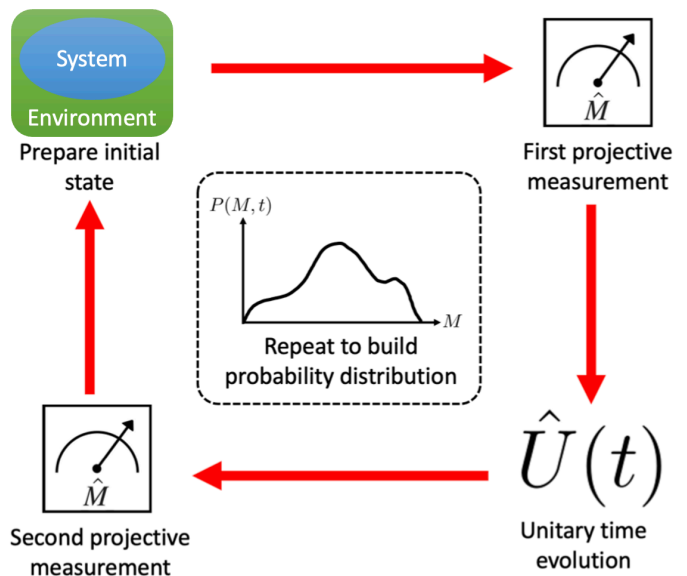


FIG. 1. Schematic of the two-point measurement protocol. First we prepare an initial state of the system, which we assumed is coupled to a thermal environment. We then perform a projective measurement onto the eigenbasis of some observable,  $\hat{M}$ , and allow the composite system to evolve unitarily for a time  $t$ , before performing another projective measurement onto the eigenbasis of  $\hat{M}$ . We take the difference of the two measurement outcomes,  $M$ , to be the value of the quantity we want to measure (in this case, heat). This value is stochastic, so we repeat the protocol many times in order to build a probability distribution,  $P(M, t)$ . The objective of this work is to test different definitions of heat through the choice of the operator,  $\hat{M}$ .

tity  $M$ . Following Esposito *et al.* [2], we can write the CF as

$$\Phi(\chi, t) = \text{Tr}[\hat{\rho}(\chi, t)], \quad (2)$$

where we have defined the generalised density operator

$$\hat{\rho}(\chi, t) = \hat{U}_{\frac{\chi}{2}}(t) e^{-i\frac{\chi}{2}\hat{M}} \bar{\rho}_0 e^{i\frac{\chi}{2}\hat{M}} \hat{U}_{-\frac{\chi}{2}}^\dagger(t), \quad (3)$$

and have made use of a generalised time evolution operator

$$\hat{U}_\chi(t) = e^{i\chi\hat{M}} \hat{U}(t) e^{-i\chi\hat{M}}. \quad (4)$$

In Eq. (3),  $\bar{\rho}_0 = \sum_{m_0} |m_0\rangle\langle m_0| \hat{\rho}(0) |m_0\rangle\langle m_0|$  is the initial state of the composite system after being averaged over the initial measurement outcomes of  $\hat{M} = \sum_{m_0} m_0 |m_0\rangle\langle m_0|$ . Applying a partial trace over the environment degrees of freedom in Eq. (2) gives

$$\Phi(\chi, t) = \text{Tr}_S[\hat{\rho}_S(\chi, t)], \quad (5)$$

where we have defined the reduced generalised density operator for the system as  $\hat{\rho}_S(\chi, t) = \text{Tr}_E[\hat{\rho}(\chi, t)]$ . By deriving an equation of motion for  $\hat{\rho}_S(\chi, t)$  and taking the trace, we can generate the full probability distribution for a given observable  $\hat{M}$  by inverting the Fourier transform.

As shown in Ref. [5], in the limit of weak system-environment interactions, we are able to derive a Born-Markov master equation describing the evolution of the reduced generalised density operator,

$$\frac{d}{dt}\hat{\rho}_S(\chi, t) = \mathcal{L}_S(\chi)\hat{\rho}_S(\chi, t), \quad (6)$$

where  $\mathcal{L}_S(\chi)$  is the  $\chi$ -dressed Liouville superoperator [27] that describes both the coherent dynamics and the effect of the environment on the reduced generalised density operator. Solving this master equation with an appropriate initial condition,  $\hat{\rho}_S(\chi, 0)$ , yields the CF.

## B. Reaction Coordinate Mapping

Here we are interested in studying heat exchange beyond the Born-Markov limit. We consider the spin-boson model,

$$\hat{H} = \frac{\epsilon}{2}\hat{\sigma}_z + \frac{\Delta}{2}\hat{\sigma}_x + \hat{\sigma}_z \otimes \sum_k f_k(\hat{c}_k^\dagger + \hat{c}_k) + \sum_k \nu_k \hat{c}_k^\dagger \hat{c}_k, \quad (7)$$

where  $\epsilon$  is the energy gap between basis states  $|e\rangle$  and  $|g\rangle$  of a two-level system (TLS), and  $\Delta$  is the tunneling between them. The  $k^{\text{th}}$ -mode of the bosonic environment has creation (annihilation) operators  $\hat{c}_k^\dagger$  ( $\hat{c}_k$ ), with energy  $\nu_k$ , and system-mode coupling strength  $f_k$ . The system-environment coupling is fully described by the spectral density function,  $J(\nu) = \sum_k |f_k|^2 \delta(\nu - \nu_k)$ .

There has been significant effort in developing numerical methods to describe both the dynamics and thermodynamics of the spin-boson model. Notable examples include those based on discrete-time path integral [28, 29] and their expression as tensor networks [30, 31], hierarchical equations of motion [32–34], and chain mapping methods [35, 36]. While such techniques can be used to obtain numerically exact results in many regimes, they are computationally demanding and can be challenging to interpret. In contrast, nonperturbative master equation techniques, such as the polaron theory [37] and its variational extensions [38, 39] are intuitive and computational cheap, though often at the expense of restricted applicability. The nonperturbative method we use in this work is the reaction coordinate mapping [13, 15, 19, 21].

In the RC approach, a mapping is applied to the spin-boson model which extracts a collective coordinate from the environment (from now on the original environment is referred to as the full environment), which we call the *reaction coordinate* (RC). The TLS, RC and their interaction are incorporated into an *extended system* (ES), and the remaining environment degrees of freedom are collected into *residual environment* (RE), which couples to the extended system through the RC. For a detailed discussion of the RC mapping we refer the reader to Refs. [15, 21].

We introduce a unitary operator,  $\hat{\mathcal{R}}$ , which performs the mapping. Upon applying the RC mapping, we obtain the Hamiltonian,

$$\hat{H}_{\mathcal{R}} = \hat{\mathcal{R}}\hat{H}\hat{\mathcal{R}}^\dagger = \hat{H}_{\text{ES}} + \hat{H}_{\text{I}} + \hat{H}_{\text{RE}}, \quad (8)$$

$$\hat{H}_{\text{ES}} = \frac{\epsilon}{2}\hat{\sigma}_z + \frac{\Delta}{2}\hat{\sigma}_x + \Omega\hat{a}^\dagger\hat{a} + \lambda\hat{\sigma}_z(\hat{a}^\dagger + \hat{a}), \quad (9)$$

$$\hat{H}_{\text{I}} = (\hat{a}^\dagger + \hat{a}) \sum_k g_k(\hat{b}_k^\dagger + \hat{b}_k) + (\hat{a}^\dagger + \hat{a})^2 \sum_k \frac{g_k^2}{\omega_k}, \quad (10)$$

$$\hat{H}_{\text{RE}} = \sum_k \omega_k \hat{b}_k^\dagger \hat{b}_k. \quad (11)$$

Here, Eq. (9) is the extended system Hamiltonian, where the RC has frequency  $\Omega$ , and creation (annihilation) operators  $\hat{a}^\dagger$  ( $\hat{a}$ ), and it is coupled to the TLS with strength  $\lambda$ . Eq. (10) is the interaction between the RC and the residual environment [40] with RC-mode coupling strength  $g_k$ , and Eq. (11) is the residual environment Hamiltonian with modes of frequency  $\omega_k$ , and creation (annihilation) operators  $\hat{b}_k^\dagger$  ( $\hat{b}_k$ ).

For the spectral density describing the TLS-full environment interaction we choose an underdamped Drude-Lorentz form, describing a peak of width  $\Gamma$ , centered at  $\omega_0$ , with dimensionless coupling strength  $\alpha$ :

$$J_{\text{UD}}(\omega) = \frac{\alpha\Gamma\omega_0^2\omega}{(\omega_0^2 - \omega^2)^2 + (\Gamma\omega)^2}. \quad (12)$$

Upon applying the RCM the spectral density describing the extended system-residual environment interaction becomes Ohmic,

$$J_{\text{RC}}(\omega) = \sum_k |g_k|^2 \delta(\omega - \omega_k) = \gamma\omega, \quad (13)$$

with the coupling strength between the ES and RE being  $\gamma$ . A hard cutoff of  $\omega_{\text{cut}} = 10\omega_0$ , is added to the unmapped and mapped spectral densities in later numerical simulations.

For sufficiently weak coupling to the RE (small  $\gamma$ ) we can derive a Born-Markov master equation for the extended system state  $\hat{\rho}_{\text{ES}}(t)$ . After solving this reaction coordinate master equation, we can trace out the RC degrees of freedom to obtain the state of the TLS:  $\hat{\rho}_S(t) = \text{Tr}_{\text{RC}}[\hat{\rho}_{\text{ES}}(t)]$ . The RCME accurately captures both non-Markovian and strong coupling effects. To confirm this, we present a comparison of an exactly solvable limit of the spin-boson model (the independent boson model for which  $\Delta = 0$  [27]) with the RCME in App. A, demonstrating excellent agreement across all timescales tested.

## C. Heat counting in the reaction coordinate formalism

We now apply the RCM to heat counting statistics. Let us begin with the CF to count energetic changes in

the full environment, given by

$$\Phi_{\text{F}}^{\text{rc}}(\chi, t) = \text{Tr} \left[ e^{i\chi \hat{H}_{\text{E}}} \hat{U}(t) e^{-i\chi \hat{H}_{\text{E}}} \bar{\rho}_0 \hat{U}^\dagger(t) \right], \quad (14)$$

where we perform projective measurements onto  $\hat{M} = \hat{H}_{\text{E}}$ . We make the assumption that the initial state is uncorrelated,  $\hat{\rho}(0) = \hat{\rho}_{\text{S}}(0) \otimes \hat{\rho}_{\text{E}}$ , where  $\hat{\rho}_{\text{E}}$  is the Gibbs state  $\hat{\rho}_{\text{E}} = \exp[-\beta \hat{H}_{\text{E}}] / \mathcal{Z}_{\text{E}}$ , where  $\mathcal{Z}_{\text{E}} = \text{Tr}[\exp[-\beta \hat{H}_{\text{E}}]]$  is the partition function, with inverse bath temperature  $\beta$ . For this initial state we have  $\bar{\rho}_0 = \hat{\rho}(0)$ .

By resolving the identity as  $\mathcal{I} = \hat{\mathcal{R}}^\dagger \hat{\mathcal{R}}$  we can rewrite the CF in Eq. (14) as

$$\Phi_{\text{F}}^{\text{rc}}(\chi, t) = \text{Tr} \left[ e^{i\chi \hat{\mathcal{R}}^\dagger \hat{H}_{\text{E}} \hat{\mathcal{R}}} \hat{U}_{\hat{\mathcal{R}}}(t) e^{-i\chi \hat{\mathcal{R}}^\dagger \hat{H}_{\text{E}} \hat{\mathcal{R}}} \hat{\mathcal{R}}^\dagger \hat{\rho}(0) \hat{\mathcal{R}} \hat{U}_{\hat{\mathcal{R}}}^\dagger(t) \right]. \quad (15)$$

We have also defined the time evolution operator in the reaction coordinate frame as

$$\hat{U}_{\hat{\mathcal{R}}}(t) = \hat{\mathcal{R}} \exp[-i\hat{H}t] \hat{\mathcal{R}}^\dagger = \exp[-i\hat{H}_{\hat{\mathcal{R}}}t], \quad (16)$$

where  $\hat{H}_{\hat{\mathcal{R}}}$  is the Hamiltonian given in Eq. (8). We assume that the RCM is performed such that the interaction between the RC and RE is weak, i.e.  $\hat{H}_{\text{I}} \approx 0$ . Performing the RCM and making the weak coupling approximation gives us

$$\begin{aligned} \Phi_{\text{F}}^{\text{rc}}(\chi, t) \approx & \text{Tr} \left[ e^{i\chi(\hat{H}_{\text{RC}} + \hat{H}_{\text{RE}})} \hat{U}_{\hat{\mathcal{R}}}(t) e^{-i\chi(\hat{H}_{\text{RC}} + \hat{H}_{\text{RE}})} \right. \\ & \left. \times \hat{\rho}_{\text{S}}(0) \otimes \hat{\rho}_{\text{RC}} \otimes \hat{\rho}_{\text{RE}} \hat{U}_{\hat{\mathcal{R}}}^\dagger(t) \right], \quad (17) \end{aligned}$$

where in the same approximation we have

$$\hat{\mathcal{R}}^\dagger \hat{\rho}_{\text{E}} \hat{\mathcal{R}} \approx \hat{\rho}_{\text{RC}} \otimes \hat{\rho}_{\text{RE}}, \quad (18)$$

where  $\hat{\rho}_{\text{RC}}$  ( $\hat{\rho}_{\text{RE}}$ ) is the Gibbs state of the RC (RE). Using the cyclic property of the trace we rewrite the CF as

$$\Phi_{\text{F}}^{\text{rc}} = \text{Tr} \left[ e^{i\chi \hat{H}_{\text{RC}}} \hat{\rho}(\chi, t) \right], \quad (19)$$

where we have defined the generalised density operator as

$$\begin{aligned} \hat{\rho}(\chi, t) = & e^{i\frac{\chi}{2} \hat{H}_{\text{RE}}} \hat{U}_{\hat{\mathcal{R}}}(t) e^{-i\chi(\hat{H}_{\text{RC}} + \hat{H}_{\text{RE}})} \\ & \times \hat{\rho}_{\text{S}}(0) \otimes \hat{\rho}_{\text{RC}} \otimes \hat{\rho}_{\text{RE}} \hat{U}_{\hat{\mathcal{R}}}^\dagger(t) e^{i\frac{\chi}{2} \hat{H}_{\text{RE}}}. \quad (20) \end{aligned}$$

By taking the time derivative of this generalised density operator and moving into the interaction picture with respect to  $\hat{H}_{\text{ES}} + \hat{H}_{\text{RE}}$  we find an equation of motion which resembles the Liouville-von Neumann equation [27]

$$\frac{d}{dt} \tilde{\rho}(\chi, t) = -i \left( \tilde{H}_{\text{I}}(\chi, t) \tilde{\rho}(\chi, t) - \tilde{\rho}(\chi, t) \tilde{H}_{\text{I}}(-\chi, t) \right), \quad (21)$$

where

$$\tilde{H}_{\text{I}}(\chi, t) = e^{i\frac{\chi}{2} \hat{H}_{\text{RE}}} e^{i(\hat{H}_{\text{ES}} + \hat{H}_{\text{RE}})t} \hat{H}_{\text{I}} e^{-i(\hat{H}_{\text{ES}} + \hat{H}_{\text{RE}})t} e^{-i\frac{\chi}{2} \hat{H}_{\text{RE}}}. \quad (22)$$

We use this equation as a basis to derive a master equation which treats the Hamiltonian of the extended system exactly and the effect of the residual environment on the extended system up to second order in  $\hat{H}_{\text{I}}$ , leading us to the *heat-counting reaction coordinate master equation* (HC-RCME)

$$\frac{d}{dt} \hat{\rho}_{\text{ES}}(\chi, t) = \mathcal{L}_{\text{ES}}(\chi) [\hat{\rho}_{\text{ES}}(\chi, t)]. \quad (23)$$

Details of the form of  $\mathcal{L}_{\text{ES}}(\chi)$  can be found in Appendix B.

Notice, however, that the RCM gives us two possible environments to use within the TPMP: There is the environment prior to the mapping which includes all phonon degrees of freedom, the *full environment* (FE); and there is the environment after the mapping, the residual environment (RE), which is weakly coupled to the extended system. Performing the projective measurements onto these two Hamiltonians results in two different CFs and thus definitions of heat, which we can compare. When counting only on the RE we take  $\hat{M} = \hat{\mathcal{R}}^\dagger \hat{H}_{\text{RE}} \hat{\mathcal{R}}$  [41], which leads to

$$\Phi_{\text{R}}^{\text{rc}}(\chi, t) = \text{Tr} [\hat{\sigma}_{\text{ES}}(\chi, t)]. \quad (24)$$

The two generalised density operators  $\hat{\rho}_{\text{ES}}(\chi, t)$  and  $\hat{\sigma}_{\text{ES}}(\chi, t)$  both obey the HC-RCME but have different initial conditions, being

$$\hat{\rho}_{\text{ES}}(\chi, 0) = \hat{\rho}_{\text{S}}(0) \otimes \frac{e^{-(\beta+i\chi)\Omega\hat{a}^\dagger\hat{a}}}{\text{Tr} [e^{-\beta\Omega\hat{a}^\dagger\hat{a}}]}, \quad (25)$$

and

$$\hat{\sigma}_{\text{ES}}(\chi, 0) = \hat{\rho}_{\text{S}}(0) \otimes \frac{e^{-\beta\Omega\hat{a}^\dagger\hat{a}}}{\text{Tr} [e^{-\beta\Omega\hat{a}^\dagger\hat{a}}]} = \hat{\rho}_{\text{S}}(0) \otimes \hat{\rho}_{\text{RC}}. \quad (26)$$

where  $\hat{\rho}_{\text{S}}(0)$ , is the initial state of the TLS, which we take to be  $\hat{\rho}_{\text{S}}(0) = |+\rangle\langle+|$  throughout this work, where  $|+\rangle = \frac{1}{\sqrt{2}}(|e\rangle + |g\rangle)$ .

While the HC-RCME can in principle be used to investigate the full spin-boson model, in order to investigate the difference in system-environment partitions on the resulting heat statistics, it is instructive to consider the independent boson model (IBM). Following Popovic *et al* [42], we are able to find an analytic expression for the CF describing energetic changes in the FE, given by

$$\begin{aligned} \Phi_{\text{F}}^{\text{ex}}(\chi, t) = & \exp \left[ -2 \int_0^\infty d\omega \frac{J_{\text{UD}}(\omega)}{\omega^2} (1 - \cos(\omega t)) \right. \\ & \left. \times \left( \coth \left( \frac{\beta\omega}{2} \right) (1 - \cos(\omega\chi)) - i \sin(\omega\chi) \right) \right]. \quad (27) \end{aligned}$$

A similar expression for changes in the RE is not available since this definition requires performing the RCM, and cannot be found analytically.

### III. RESULTS

#### A. Characteristic function

Our results are based around three different CFs. Two of which calculate energetic changes in the full environment Hamiltonian, using either the exact or approximate (i.e. HC-RCME) methods of calculating the dynamics of the generalised density operator. The other CF counts energetic changes in the residual environment Hamiltonian and is found using the approximate method of calculating these dynamics. We use subscripts to denote the definition of heat the CF counts: ‘F’ for full environment and ‘R’ for residual environment. The superscript describes the method through which the generalised density operator dynamics are calculated: ‘rc’ for the HC-RCME and ‘ex’ for the analytical dynamics from the IBM.

In Fig. 2 we plot the real (left) and imaginary (right) parts of  $\Phi_{\text{F}}^{\text{ex}}$  (green solid) and  $\Phi_{\text{F}}^{\text{rc}}$  (orange stars, dashed), both of which count energetic changes in the full environment Hamiltonian. We see excellent agreement between these two CFs close to  $\chi = 0$ , with deviations at larger values of  $\chi$  shown in the inset. The analytic result shows decaying repetitions of the main feature centred around  $\chi = 0$ , whereas the HC-RCME captures this main feature but lacks the subsequent decay for larger  $\chi$  values. Also shown in Fig. 2 is the characteristic function which counts energetic changes in the residual environment Hamiltonian,  $\Phi_{\text{R}}^{\text{rc}}$  (purple circles, dotted). We see similar qualitative behaviour between  $\Phi_{\text{F}}^{\text{rc}}$  and  $\Phi_{\text{R}}^{\text{rc}}$ , in that they repeat their feature centered at  $\chi = 0$ , with no decay as we increase  $\chi$ .

It is clear that there are quantitative differences in the CFs when counting only on the residual environment rather than the full environment. The physical meaning behind these differences are not immediately obvious from these results alone. In the following section we calculate the first two moments of the probability distributions associated with these CFs, calculated by evaluating derivatives of the CFs at  $\chi = 0$ .

#### B. Statistical Moments

By taking derivatives of the CFs and evaluating them at  $\chi = 0$ , we can find the moments of the probability distribution associated with them. In particular, the  $n^{\text{th}}$  moment is given by

$$\langle Q^n \rangle(t) = (-i)^n \left. \frac{d^n}{d\chi^n} \Phi(\chi, t) \right|_{\chi=0}. \quad (28)$$

Therefore, the excellent agreement between  $\Phi_{\text{F}}^{\text{ex}}$  and  $\Phi_{\text{F}}^{\text{rc}}$  around  $\chi = 0$  shown in Fig. 2 implies that the HC-RCME can accurately capture the statistical moments of the probability distributions for the two definitions of heat, which we study now.

We can find analytic forms for the moments of the full environment heat distribution by applying Eq. (28) to Eq. (27), giving

$$\langle Q_{\text{F}}^{\text{ex}}(t) \rangle = 2 \int_0^{\infty} d\omega \frac{J_{\text{UD}}(\omega)}{\omega} (1 - \cos(\omega t)), \quad (29)$$

for the mean, and

$$\text{var}[Q_{\text{F}}^{\text{ex}}(t)] = 2 \int_0^{\infty} d\omega J_{\text{UD}}(\omega) \coth\left(\frac{\beta\omega}{2}\right) (1 - \cos(\omega t)), \quad (30)$$

for the variance.

To calculate the mean and variance predicted by the HC-RCME,  $\Phi_{\text{F}}^{\text{rc}}$  and  $\Phi_{\text{R}}^{\text{rc}}$ , we follow the finite difference method used by Popovic *et al* [42]. By choosing a small value of the counting parameter  $\chi_\epsilon$ , we find the mean as

$$\langle Q_i^{\text{rc}}(t) \rangle = \frac{\text{Im}[\Phi_i^{\text{rc}}(\chi_\epsilon, t)]}{\chi_\epsilon} + \mathcal{O}(\chi_\epsilon), \quad (31)$$

and the variance as

$$\text{var}[Q_i^{\text{rc}}(t)] = \frac{2 - 2\text{Re}[\Phi_i^{\text{rc}}(\chi_\epsilon, t)]}{\chi_\epsilon^2} - \langle Q_i^{\text{rc}}(t) \rangle^2 + \mathcal{O}(\chi_\epsilon^2), \quad (32)$$

where  $i = \text{F}$  for the full environment definition and  $i = \text{R}$  for the residual environment definition. In the above  $\mathcal{O}(x)$  represents error of order  $x$ .

In Fig. 3 (top) we plot the mean energy change of the full environment, calculated using the exact method ( $\langle Q_{\text{F}}^{\text{ex}} \rangle$ ) (green solid) and the HC-RCME method ( $\langle Q_{\text{F}}^{\text{rc}} \rangle$ ) (orange stars, dashed), as well as the mean energy change of the residual environment ( $\langle Q_{\text{R}}^{\text{rc}} \rangle$ ) (purple solid). We show both a short (left) and a long (right) timescale.

We see that the HC-RCME accurately describes the mean energy change of the full environment. Interestingly, this demonstrates large oscillations, which can be intuitively explained using the RCM: The TLS strongly couples to the RC, which captures the long memory effects of the full environment. This leads to a coherent exchange of energy and information between the TLS and RC, suggesting that ‘heat’, as defined by the change in energy of the full environment, is not irreversibly lost to the environment, but can re-excite [43] the system leading to coherent oscillations.

This contrasts with the mean heat predicted by counting on only the residual environment, which contains heavily suppressed oscillations, suggesting that the energy is irreversibly lost to the residual environment. This behaviour is more in keeping with the classical definition of heat, which is understood to be the entropy increasing changes in energy, and which flows in a unidirectional manner from a hot body to a cold body.

These differences are also reflected in Fig. 3 (bottom), where we plot the variances associated with the CFs.

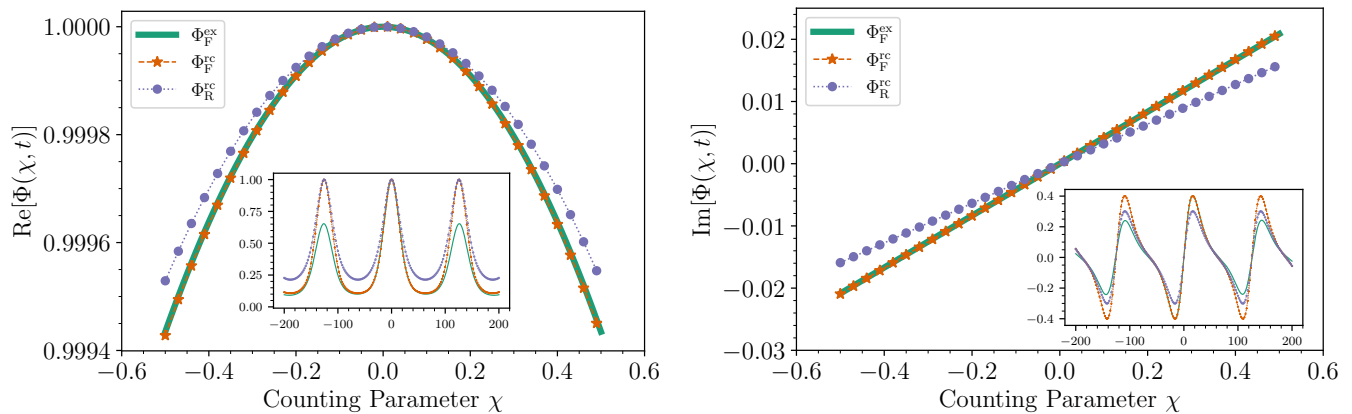


FIG. 2. Real (left) and imaginary (right) parts of the CFs of heat transfer in the independent boson model. We compare an exact analytic solution  $\Phi_F^{\text{ex}}$  (green solid) with the CF which uses the HC-RCME method  $\Phi_F^{\text{rc}}$  (orange stars, dashed) both of which define heat as changes in the energy of the full environment. Together with this we show the CF which defines heat as energetic changes in the Hamiltonian of the residual environment,  $\Phi_R^{\text{rc}}$  (purple circles, dotted). The CF is evaluated at a time when the system coherence is in the steady state,  $t = 1000\text{ps}$ . The main curves show the CFs close to  $\chi = 0$ , where we see excellent agreement between the analytic and RC solution, suggesting the HC-RCME can capture the statistics of the full environment. The insets show a larger range of counting parameters, where we see deviations between the analytic and RC results for the full environment. The TLS energy splitting is  $\epsilon = 2\text{eV}$  and begins in the state  $\hat{\rho}_S(0) = |+\rangle\langle +|$  (where  $|+\rangle = \frac{1}{\sqrt{2}}(|e\rangle + |g\rangle)$ ), the environment spectral density parameters are  $\alpha = 0.1$ ,  $\Gamma = 0.001\text{eV}$ ,  $\omega_0 = 0.05\text{eV}$ , and the environment is at  $T = 300\text{K}$ , with  $M_{\text{RC}} = 20$  states simulated in the RC. These parameters are used throughout this work.

Once again, we see excellent agreement between the exact treatment and the HC-RCME when counting on the full environment. Similar to the case of the mean value, we see both quantitative and qualitative differences in the variance when counting only on the residual environment, with oscillations suppressed, and the overall variance being less than the full environment definition of heat. The variance of heat is expected to increase with time, which suggests that the residual environment definition is more in keeping in the non-Markovian regime.

### C. Ergotropy

The coherent oscillations observed in Fig. 3 for both methods of calculating the mean energy change of the full environment,  $\langle Q_F^{\text{ex}} \rangle$  and  $\langle Q_F^{\text{rc}} \rangle$ , suggests that there is a work-like contribution within the definition of heat which counts energetic changes in the full environment Hamiltonian. The RC method provides us with a unique insight into this behaviour, providing an avenue to calculate the ergotropy [25, 44, 45] of the TLS, which treats all energy emitted into the environment as heat (i.e. the full environment paradigm referenced above), as well as the extended system, treating the RC as a potential work source. The ergotropy is defined as the maximum amount of work we can extract unitarily from a quantum state, and for the two environment partitions can be defined as,

$$\mathcal{E}(\hat{\rho}_S, \hat{H}_S) = \text{Tr} \left[ \hat{H}_S \hat{\rho}_S \right] - \min_{\hat{U}} \text{Tr} \left[ \hat{H}_S \hat{U} \hat{\rho}_S \hat{U}^\dagger \right], \quad (33)$$

for the TLS, and for the extended system as

$$\mathcal{E}(\hat{\rho}_{\text{ES}}, \hat{H}_{\text{ES}}) = \text{Tr} \left[ \hat{H}_{\text{ES}} \hat{\rho}_{\text{ES}} \right] - \min_{\hat{V}} \text{Tr} \left[ \hat{H}_{\text{ES}} \hat{V} \hat{\rho}_{\text{ES}} \hat{V}^\dagger \right], \quad (34)$$

where the minimisation is taken over all unitaries acting on the Hilbert space of the TLS or extended system. The time dependence of the ergotropies and states have been omitted from the above definition for ease of reading. This minimisation is satisfied through a unitary transformation which takes the state to its passive counterpart, from which no further work can be extracted [25]. By diagonalising the state as

$$\hat{\rho} = \sum_j r_j |r_j\rangle \langle r_j| \quad (35)$$

such that  $r_j > r_{j+1}$ , and diagonalising the Hamiltonian as

$$\hat{H} = \sum_k \epsilon_k |\epsilon_k\rangle \langle \epsilon_k| \quad (36)$$

such that  $\epsilon_k < \epsilon_{k+1}$  the ergotropy is given by

$$\mathcal{E}(\hat{\rho}, \hat{H}) = \sum_{jk} r_j \epsilon_k \left( | \langle r_j | \epsilon_k \rangle |^2 - \delta_{jk} \right), \quad (37)$$

where it is essential that the ordering of the eigenvalues  $\epsilon_k$  and populations  $r_j$  (and the eigenvectors associated with them) is correct, due to the presence of the delta function.

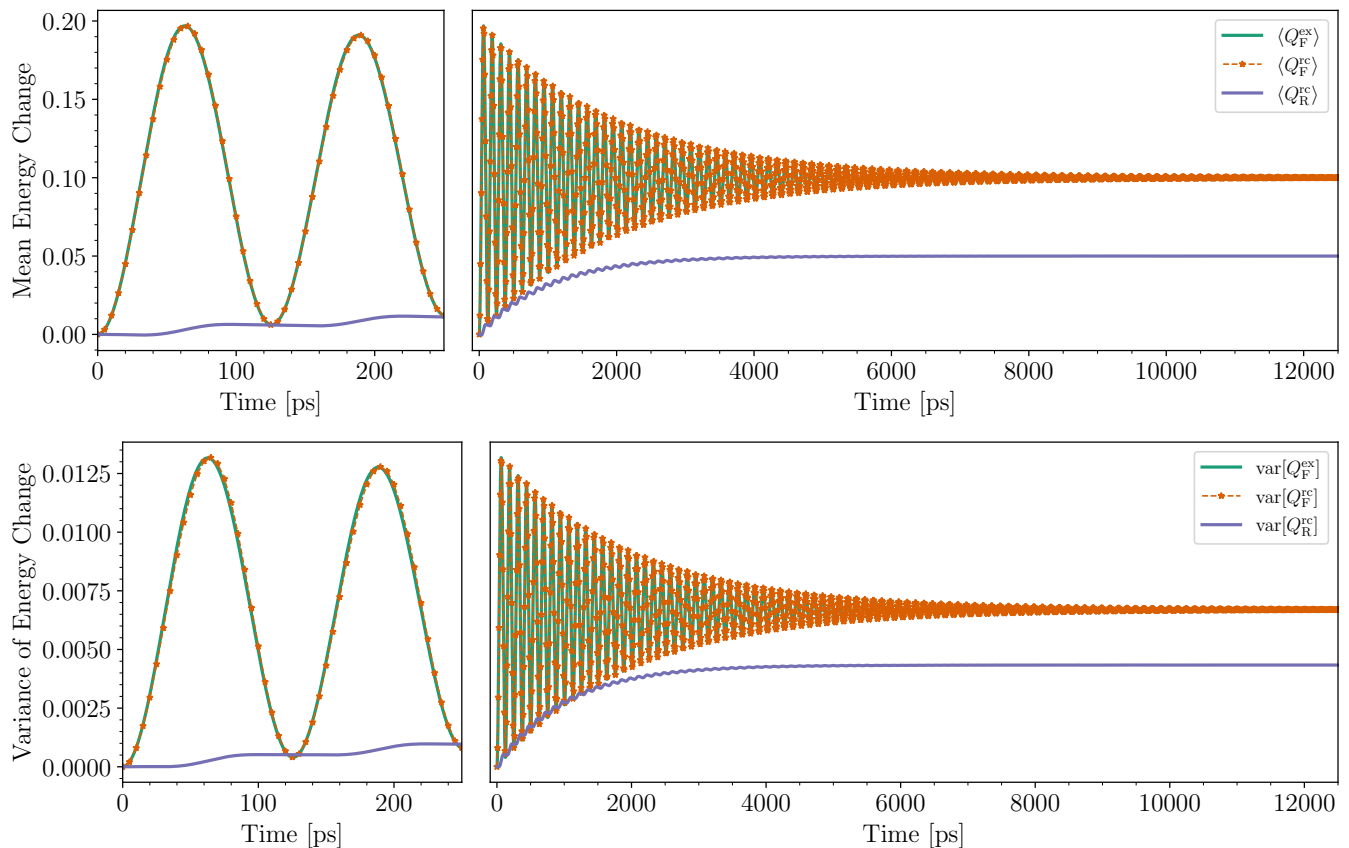


FIG. 3. Mean (top) and variance (bottom) of heat transfer in the independent boson model, as defined by changes in the energy of the full environment, calculating using the analytic result (green solid) and using the HC-RCME (orange stars, dashed), and changes in the energy of the residual environment (purple solid). We show both short time (left) and long time (right) behaviour of the first two statistical moments, where we see significant qualitative difference in the mean and variance of energy changes of the full environment and residual environment. The small value of the counting parameter we use to calculate the moments in Eq.(31) and Eq.(32) is  $\chi_\epsilon = 0.005$ , and all other parameters are those given in Figure 2.

In Fig. 4 we plot the ergotropies of the TLS state and extended system state, when starting the TLS in the state  $\hat{\rho}_S(0) = |+\rangle\langle +|$  and the RC in the Gibbs state.

At  $t = 0$  the TLS ergotropy (orange, dashed) is the amount of extractable energy by unitarily transforming from  $|+\rangle$  to the ground state  $|g\rangle$ , as expected. We then see a sharp decrease in ergotropy followed by decaying recurrences, which are in phase with the decoherence and recoherences of the TLS induced by the non-Markovian interaction with the full environment, as seen in Fig. 5. This is explained by coherence in the energy eigenbasis of a system being able to contribute to ergotropy [26, 46, 47]. When calculating the ergotropy of the TLS state, we assume we have complete control over the TLS, but no control over the full environment. During decoherence the system has reduced contributions to its ergotropy in the form of coherence terms. During the re-coherence process, the environment generates coherence in the TLS (in ever smaller quantities), providing an increase in the extractable work.

When considering the ergotropy of the extended sys-

tem, we see that the presence of the RC increases ergotropy by providing access to coherence that are otherwise lost to the full environment. Notably, the ergotropy of the extended system begins at a larger value than that of the TLS, despite the RC beginning in the Gibbs state. While the Gibbs state is passive with respect to the RC Hamiltonian, the presence of the interaction term between the TLS-RC means the Gibbs state is no longer passive, providing an increase in the amount of extractable work. This interaction maintains coherence within the extended system, explaining the (relatively) constant ergotropy. However, a gradual decay occurs in the extended system's ergotropy resulting from the weak interaction between the RC and the (infinite) residual environment, causing slow, and irreversible decoherence and dissipation in the extended system.

These results appear to show that the RC is a viable work source, at least in theory. Therefore, if work and heat are to be defined as separate and distinct components of a system's internal energy change, definitions of heat should not include energetic changes within the RC.

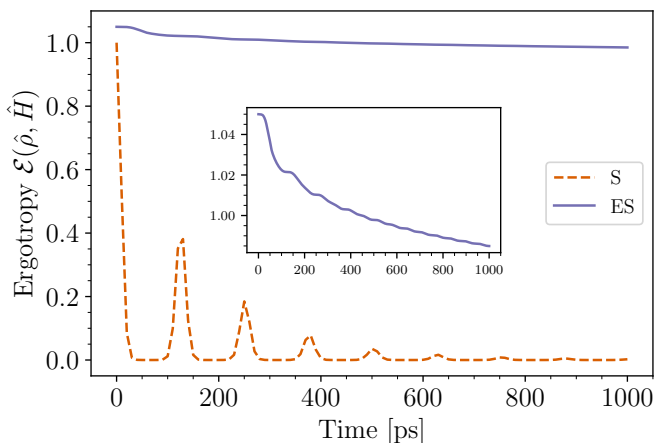


FIG. 4. Ergotropy of the TLS (orange dashed) and extended system (purple solid). Decay and periodic revivals of the system ergotropy are due to decoherence and recoherence of the system, respectively. The extended system ergotropy remains higher than the system’s for all times, due to access of this coherence through the RC. Decay of the extended system ergotropy is due to its weak interaction with the residual environment, which causes irreversible loss of coherence.

This gives further evidence to support using the definition of heat as energetic changes in the residual environment Hamiltonian in this parameter regime.

#### IV. DISCUSSION

We have used the two-point measurement protocol to study the full counting statistics of energetic changes in the spin-boson model in the non-Markovian regime. We employ the reaction coordinate (RC) formalism which

not only accounts for system-environment correlations through the RC, enabling us to study energetic changes in the environment in strong coupling regimes, but also allows us to investigate how different system-environment partitions impact the definition of heat in open quantum systems.

Notably, we find that a naïve definition of heat, in which all energy changes of an environment is categorised as heat, overlooks significant work-like contributions present in the system-environment interactions, which leads to coherent oscillations in both the average and variance of these energetic changes. The RC formalism however, allows us to use an alternative definition of heat in which only energetic changes of residual environment are considered as heat. With this definition, coherent oscillation in the mean and variance heat are heavily suppressed, suggesting heat in this case is truly an irreversible (i.e. entropy increasing) process. This is supported by considering the ergotropy for both the TLS and extended system. Access to the RC results in an increased ergotropy (unitarily extractable work), suggesting that a definition of heat should not contain energetic changes of the RC.

This work demonstrates that defining heat as changes in the energy of the residual environment, as characterized by the RCM, aligns with the classical intuition of heat: entropy-increasing changes in internal energy that are distinct from work. Recent research [48] supports this conclusion, revealing that peaks in the spectral density of a supposedly thermal environment can enable it to partially function as a work reservoir. Combined with our findings, this suggests that assumptions about the interaction between an open quantum system and a thermal environment must be made cautiously. It is particularly crucial to consider the structure of the environment’s spectral density when evaluating energy transfer and making the distinction between heat and work.

#### Appendix A: Benchmarking Dynamics

Here we show that the RCME (HC-RCME with  $\chi = 0$ ) is able to track system properties accurately. In Fig. 5 we plot the dynamics of the system coherence  $\langle \hat{\sigma}_x(t) \rangle$  on both a short (left) and long (right) timescale, by solving the RCME (blue) and the analytic result from the IBM (black dots). We see that the RCME is able to track the system coherence dynamics very well with  $M_{RC} = 20$  energy levels being simulated in the RC. The TLS energy splitting is  $\epsilon = 2\text{eV}$ , the environment spectral density parameters are  $\alpha = 0.1$ ,  $\Gamma = 0.001\text{eV}$ ,  $\omega_0 = 0.05\text{eV}$ , and the environment is at a temperature  $T = 300\text{K}$ . We use these parameters throughout this work. The system coherence shows decaying oscillations on a short timescale Fig.5 (left), with periodic recoherences on longer timescales, which themselves decay in time Fig.5 (right). These recoherences are a result of the sharply peaked form of the full environment spectral density, and indicate that we are working in a regime where the standard Born-Markov master equation would fail, as it is unable to predict recoherences of the system.

#### Appendix B: Generalised master equation in the Reaction Coordinate frame

The interaction Hamiltonian in Eq. (10) can be written as  $\hat{H}_I = \hat{A} \otimes \hat{B}$ , where  $\hat{A}$  and  $\hat{B}$  are operators on the Hilbert spaces of the extended system and residual environment, respectively. We ignore the counter term since it does not contribute to the master equation we are about to derive, other than through a shift in energies. Transforming this



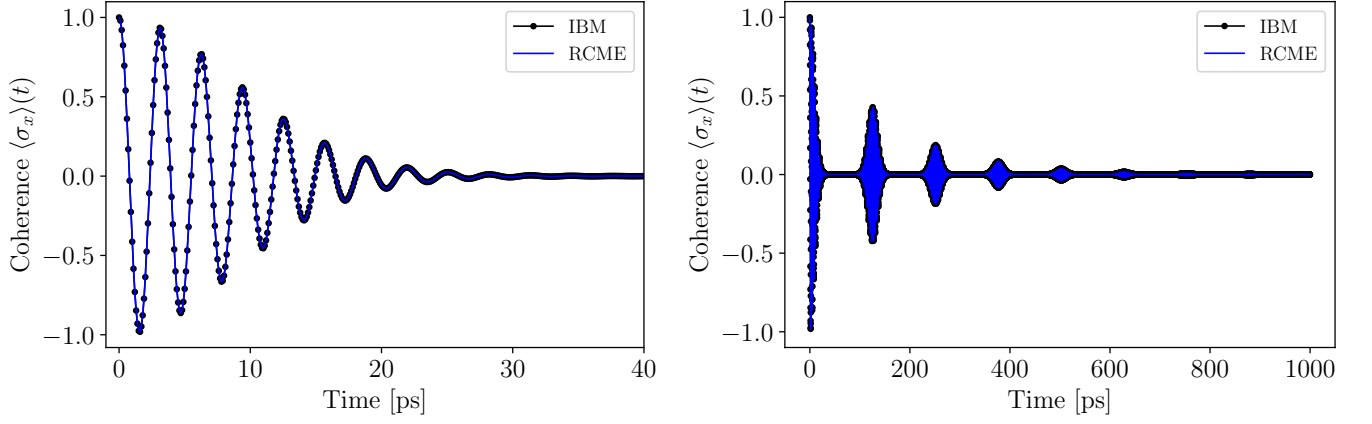


FIG. 5. Coherence dynamics  $\langle \hat{\sigma}_x(t) \rangle = \text{Tr}[\hat{\sigma}_x \hat{\rho}_S(t)]$  for the independent boson model, using the exact analytic result (black dots) and the reaction coordinate master equation (blue) for both a short (left) and long (right) timescale, with  $M_{\text{RC}} = 20$  energy levels. The TLS energy splitting is  $\epsilon = 2\text{eV}$  and begins in the state  $\hat{\rho}_S(0) = |+\rangle\langle +|$ , the environment spectral density parameters are  $\alpha = 0.1$ ,  $\Gamma = 0.001\text{eV}$ ,  $\omega_0 = 0.05\text{eV}$ , and the environment is at  $T = 300\text{K}$ .

interaction Hamiltonian with the counting parameter and moving into the interaction picture gives

$$\tilde{H}_1(\chi, t) = e^{i\hat{H}_{\text{ES}}t} \hat{A} e^{-i\hat{H}_{\text{ES}}t} \otimes e^{i\hat{H}_{\text{RE}}t} e^{i\frac{\chi}{2}\hat{H}_{\text{RE}}} \hat{B} e^{-i\frac{\chi}{2}\hat{H}_{\text{RE}}} e^{-i\hat{H}_{\text{RE}}t} = \tilde{A}(t) \otimes \tilde{B}(\chi, t). \quad (\text{B1})$$

Upon applying the Born-Markov approximations between the extended system and residual environment we arrive at the *heat-counting reaction coordinate master equation* (HC-RCME)

$$\begin{aligned} \frac{d}{dt} \hat{\rho}_{\text{ES}}(\chi, t) &= -i \left[ \hat{H}_{\text{ES}}, \hat{\rho}_{\text{ES}}(\chi, t) \right] - \hat{A} \hat{A}_1 \hat{\rho}_{\text{ES}}(\chi, t) + \hat{A} \hat{\rho}_{\text{ES}}(\chi, t) \hat{A}_2(\chi) + \hat{A}_3(\chi) \hat{\rho}_{\text{ES}}(\chi, t) \hat{A} - \hat{\rho}_{\text{ES}}(\chi, t) \hat{A}_4 \hat{A} \\ &= \mathcal{L}_{\text{ES}}(\chi) [\hat{\rho}_{\text{ES}}(\chi, t)]. \end{aligned} \quad (\text{B2})$$

The terms in the above equation are given by

$$\hat{A}_1 = \int_0^\infty d\tau \tilde{A}(-\tau) \langle \tilde{B}(\chi, \tau) \hat{B}(\chi) \rangle, \quad (\text{B3})$$

$$\hat{A}_2(\chi) = \int_0^\infty d\tau \tilde{A}(-\tau) \langle \tilde{B}(-\chi, -\tau) \hat{B}(\chi) \rangle, \quad (\text{B4})$$

$$\hat{A}_3(\chi) = \int_0^\infty d\tau \tilde{A}(-\tau) \langle \tilde{B}(-\chi, \tau) \hat{B}(\chi) \rangle, \quad (\text{B5})$$

$$\hat{A}_4 = \int_0^\infty d\tau \tilde{A}(-\tau) \langle \tilde{B}(-\chi, -\tau) \hat{B}(-\chi) \rangle, \quad (\text{B6})$$

where

$$\tilde{A}(-\tau) = \sum_{j,k=1}^{2M_{\text{RC}}} e^{-i\lambda_{jk}\tau} A_{jk} |\lambda_j\rangle\langle \lambda_k|, \quad (\text{B7})$$

where the extended system Hamiltonian in its spectral form is given by  $\hat{H}_{\text{ES}} = \sum_{k=1}^{M_{\text{RC}}} \lambda_k |\lambda_k\rangle\langle \lambda_k|$ , and where the  $\chi$ -dependent residual environment correlation functions are given by

$$\langle \tilde{B}(\chi, \tau) \hat{B}(\chi) \rangle = \int_0^\infty d\omega J_{\text{RC}}(\omega) \left( N(\omega) e^{i\omega\tau} + (1 + N(\omega)) e^{-i\omega\tau} \right), \quad (\text{B8})$$

$$\langle \tilde{B}(-\chi, \pm\tau) \hat{B}(\chi) \rangle = \int_0^\infty d\omega J_{\text{RC}}(\omega) \left( N(\omega) e^{\pm i\omega\tau} e^{-i\chi\omega} + (1 + N(\omega)) e^{\mp i\omega\tau} e^{i\chi\omega} \right), \quad (\text{B9})$$

$$\langle \tilde{B}(-\chi, -\tau) \hat{B}(-\chi) \rangle = \int_0^\infty d\omega J_{\text{RC}}(\omega) \left( N(\omega) e^{-i\omega\tau} + (1 + N(\omega)) e^{i\omega\tau} \right). \quad (\text{B10})$$

By making use of the Sokhotski-Plemelj theorem [27]

$$\int_0^\infty d\tau e^{-i(\omega \pm \nu)\tau} = \pi \delta(\omega \pm \nu) - i\mathcal{P} \left( \frac{1}{\omega \pm \nu} \right), \quad (\text{B11})$$

we can evaluate the time and frequency integrals. In the above,  $\delta(x - a)$  represents a Dirac delta function centred at  $x = a$ , and  $\mathcal{P}$  is the Cauchy principal value. Due to the delta function, and the fact that the spectral density and thermal occupation for bosons  $N(\omega) = (e^{\beta\omega} - 1)^{-1}$ , are ill-defined for negative frequencies, the operators Eqs. (B3)-(B6) depend on the value of  $\lambda_{mn} = \lambda_m - \lambda_n$ . Since the double sum in Eq (B7) run through every combination of eigenvalues  $(\lambda_m, \lambda_n)$ , their difference  $\lambda_{mn}$  can be positive, negative, or zero.

After evaluating these  $\tau$  integrals, ignoring the principal value terms, and taking into consideration the three possible cases for  $\lambda_{mn}$ , we end up with

$$\hat{A}_1 = \sum_{mn} \begin{cases} \pi A_{mn} J_{\text{RC}}(\lambda_{mn}) N(\lambda_{mn}) |\lambda_m\rangle\langle\lambda_n| & \text{if } \lambda_{mn} > 0, \\ \pi A_{mn} J_{\text{RC}}(|\lambda_{mn}|) (1 + N(|\lambda_{mn}|)) |\lambda_m\rangle\langle\lambda_n| & \text{if } \lambda_{mn} < 0, \\ \pi A_{mn} \gamma \beta^{-1} |\lambda_m\rangle\langle\lambda_n| & \text{if } \lambda_{mn} = 0, \end{cases} \quad (\text{B12})$$

$$\hat{A}_2(\chi) = \sum_{mn} \begin{cases} A_{mn} J_{\text{RC}}(\lambda_{mn}) (1 + N(\lambda_{mn})) e^{i\chi\lambda_{mn}} |\lambda_m\rangle\langle\lambda_n| & \text{if } \lambda_{mn} > 0, \\ \pi A_{mn} J_{\text{RC}}(|\lambda_{mn}|) N(|\lambda_{mn}|) e^{-i\chi|\lambda_{mn}|} |\lambda_m\rangle\langle\lambda_n| & \text{if } \lambda_{mn} < 0, \\ \pi A_{mn} \gamma \beta^{-1} |\lambda_m\rangle\langle\lambda_n| & \text{if } \lambda_{mn} = 0, \end{cases} \quad (\text{B13})$$

$$\hat{A}_3(\chi) = \sum_{mn} \begin{cases} \pi A_{mn} J_{\text{RC}}(\lambda_{mn}) N(\lambda_{mn}) e^{-i\chi\lambda_{mn}} |\lambda_m\rangle\langle\lambda_n| & \text{if } \lambda_{mn} > 0, \\ \pi A_{mn} J_{\text{RC}}(|\lambda_{mn}|) (1 + N(|\lambda_{mn}|)) e^{i\chi|\lambda_{mn}|} |\lambda_m\rangle\langle\lambda_n| & \text{if } \lambda_{mn} < 0, \\ \pi A_{mn} \gamma \beta^{-1} |\lambda_m\rangle\langle\lambda_n| & \text{if } \lambda_{mn} = 0, \end{cases} \quad (\text{B14})$$

$$\hat{A}_4 = \sum_{mn} \begin{cases} \pi A_{mn} J_{\text{RC}}(\lambda_{mn}) (1 + N(\lambda_{mn})) |\lambda_m\rangle\langle\lambda_n| & \text{if } \lambda_{mn} > 0, \\ \pi A_{mn} J_{\text{RC}}(|\lambda_{mn}|) N(|\lambda_{mn}|) |\lambda_m\rangle\langle\lambda_n| & \text{if } \lambda_{mn} < 0, \\ \pi A_{mn} \gamma \beta^{-1} |\lambda_m\rangle\langle\lambda_n| & \text{if } \lambda_{mn} = 0, \end{cases} \quad (\text{B15})$$

where, in order to calculate the  $\lambda_{mn} = 0$  terms, we take the limit as  $\omega \rightarrow 0$ , rather than evaluating the terms at  $\omega = 0$ . Through setting  $\chi = 0$  we recover the standard reaction coordinate master equation.

- 
- [1] Peter Talkner, Eric Lutz, and Peter Hänggi. Fluctuation theorems: Work is not an observable. *Physical Review E*, 75(5):050102, 2007.
- [2] Massimiliano Esposito, Upendra Harbola, and Shaul Mukamel. Nonequilibrium fluctuations, fluctuation theorems, and counting statistics in quantum systems. *Reviews of modern physics*, 81(4):1665, 2009.
- [3] Peter Talkner and Peter Hänggi. Colloquium: Statistical mechanics and thermodynamics at strong coupling: Quantum and classical. *Reviews of Modern Physics*, 92(4):041002, 2020.
- [4] Sai Vinjanampathy and Janet Anders. Quantum thermodynamics. *Contemporary Physics*, 57(4):545–579, 2016.
- [5] Mihail Silaev, Tero T Heikkilä, and Pauli Virtanen. Lindblad-equation approach for the full counting statistics of work and heat in driven quantum systems. *Physical Review E*, 90(2):022103, 2014.
- [6] Felix Binder, Sai Vinjanampathy, Kavan Modi, and John Goold. Operational thermodynamics of open quantum systems. *arXiv preprint quant-ph/1406.2801 v1*, 2014.

- [7] Rebecca Schmidt, M Florencia Carusela, Jukka P Pekola, Samu Suomela, and Joachim Ankerhold. Work and heat for two-level systems in dissipative environments: Strong driving and non-markovian dynamics. *Physical Review B*, 91(22):224303, 2015.
- [8] Álvaro M Alhambra, Stephanie Wehner, Mark M Wilde, and Mischa P Woods. Work and reversibility in quantum thermodynamics. *Physical Review A*, 97(6):062114, 2018.
- [9] Chris Jarzynski. Nonequilibrium work theorem for a system strongly coupled to a thermal environment. *Journal of Statistical Mechanics: Theory and Experiment*, 2004(09):P09005, 2004.
- [10] Mark T Mitchison. Quantum thermal absorption machines: refrigerators, engines and clocks. *Contemporary Physics*, 60(2):164–187, 2019.
- [11] Stephen Barnett and Paul M Radmore. *Methods in theoretical quantum optics*, volume 15. Oxford University Press, 2002.
- [12] Anthony Mark Fox. *Quantum optics: an introduction*, volume 15. Oxford University Press, USA, 2006.
- [13] Philipp Strasberg, Gernot Schaller, Neill Lambert, and Tobias Brandes. Nonequilibrium thermodynamics in the strong coupling and non-markovian regime based on a reaction coordinate mapping. *New Journal of Physics*, 18(7):073007, 2016.
- [14] Udo Seifert. First and second law of thermodynamics at strong coupling. *Physical review letters*, 116(2):020601, 2016.
- [15] Jake Iles-Smith, Neill Lambert, and Ahsan Nazir. Environmental dynamics, correlations, and the emergence of noncanonical equilibrium states in open quantum systems. *Physical Review A*, 90(3):032114, 2014.
- [16] Jake Iles-Smith, Arend G Dijkstra, Neill Lambert, and Ahsan Nazir. Energy transfer in structured and unstructured environments: Master equations beyond the born-markov approximations. *The Journal of chemical physics*, 144(4), 2016.
- [17] Henry Maguire, Jake Iles-Smith, and Ahsan Nazir. Environmental nonadditivity and franck-condon physics in nonequilibrium quantum systems. *Phys. Rev. Lett.*, 123:093601, Aug 2019.
- [18] Nicholas Anto-Sztrikacs and Dvira Segal. Capturing non-markovian dynamics with the reaction coordinate method. *Physical Review A*, 104(5):052617, 2021.
- [19] David Newman, Florian Mintert, and Ahsan Nazir. Performance of a quantum heat engine at strong reservoir coupling. *Phys. Rev. E*, 95:032139, Mar 2017.
- [20] Philipp Strasberg, Gernot Schaller, Neill Lambert, and Tobias Brandes. Nonequilibrium thermodynamics in the strong coupling and non-markovian regime based on a reaction coordinate mapping. *New Journal of Physics*, 18(7):073007, jul 2016.
- [21] Ahsan Nazir and Gernot Schaller. The reaction coordinate mapping in quantum thermodynamics. *Thermodynamics in the Quantum Regime: Fundamental Aspects and New Directions*, pages 551–577, 2018.
- [22] Nicholas Anto-Sztrikacs and Dvira Segal. Strong coupling effects in quantum thermal transport with the reaction coordinate method. *New Journal of Physics*, 23(6):063036, 2021.
- [23] Sebastian Restrepo, Javier Cerrillo, Philipp Strasberg, and Gernot Schaller. From quantum heat engines to laser cooling: Floquet theory beyond the Born-Markov approximation. *New Journal of Physics*, 20(5):053063, may 2018.
- [24] Sebastian Restrepo, Sina Böhring, Javier Cerrillo, and Gernot Schaller. Electron pumping in the strong coupling and non-Markovian regime: A reaction coordinate mapping approach. *Phys. Rev. B*, 100:035109, Jul 2019.
- [25] Armen E Allahverdyan, Roger Balian, and Th M Nieuwenhuizen. Maximal work extraction from finite quantum systems. *Europhysics Letters*, 67(4):565, 2004.
- [26] Gianluca Francica, Felix C Binder, Giacomo Guarnieri, Mark T Mitchison, John Goold, and Francesco Plastina. Quantum coherence and ergotropy. *Physical Review Letters*, 125(18):180603, 2020.
- [27] Heinz-Peter Breuer and Francesco Petruccione. *The theory of open quantum systems*. Oxford University Press, USA, 2002.
- [28] Nancy Makri and Dmitrii E Makarov. Tensor propagator for iterative quantum time evolution of reduced density matrices. i. theory. *J. Chem. Phys.*, 102(11):4600–4610, 1995.
- [29] Nancy Makri and Dmitrii E Makarov. Tensor propagator for iterative quantum time evolution of reduced density matrices. ii. numerical methodology. *J. Chem. Phys.*, 102(11):4611–4618, 1995.
- [30] Aidan Strathearn, Peter Kirton, Dainius Kilda, Jonathan Keeling, and Brendon William Lovett. Efficient non-markovian quantum dynamics using time-evolving matrix product operators. *Nature communications*, 9(1):3322, 2018.
- [31] Mathias R Jørgensen and Felix A Pollock. Exploiting the causal tensor network structure of quantum processes to efficiently simulate non-markovian path integrals. *Phys. Rev. Lett.*, 123(24):240602, 2019.
- [32] Yoshitaka Tanimura and Ryogo Kubo. Time evolution of a quantum system in contact with a nearly gaussian-markoffian noise bath. *Journal of the Physical Society of Japan*, 58(1):101–114, 1989.
- [33] Akihito Ishizaki and Yoshitaka Tanimura. Quantum dynamics of system strongly coupled to low-temperature colored noise bath: Reduced hierarchy equations approach. *Journal of the Physical Society of Japan*, 74(12):3131–3134, 2005.
- [34] Zhoufei Tang, Xiaolong Ouyang, Zhihao Gong, Haobin Wang, and Jianlan Wu. Extended hierarchy equation of motion for the spin-boson model. *The Journal of Chemical Physics*, 143(22), 2015.
- [35] Alex W Chin, Ángel Rivas, Susana F Huelga, and Martin B Plenio. Exact mapping between system-reservoir quantum models and semi-infinite discrete chains using orthogonal polynomials. *Journal of Mathematical Physics*, 51(9), 2010.
- [36] Robert Rosenbach, Javier Cerrillo, Susana F Huelga, Jianshu Cao, and Martin B Plenio. Efficient simulation of non-markovian system-environment interaction. *New Journal of Physics*, 18(2):023035, 2016.
- [37] Dara PS McCutcheon and Ahsan Nazir. Quantum dot rabi rotations beyond the weak exciton-phonon coupling regime. *New Journal of Physics*, 12(11):113042, 2010.
- [38] Dara PS McCutcheon and Ahsan Nazir. Consistent treatment of coherent and incoherent energy transfer dynamics using a variational master equation. *The Journal of chemical physics*, 135(11), 2011.
- [39] Dara PS McCutcheon, Nikesh S Dattani, Erik M Gauger, Brendon W Lovett, and Ahsan Nazir. A general approach to

quantum dynamics using a variational master equation: Application to phonon-damped rabi rotations in quantum dots. *Physical Review B—Condensed Matter and Materials Physics*, 84(8):081305, 2011.

- [40] This term includes a *counter term*, which ensures that the interaction Hamiltonian between the RC and residual environment is bounded from below.
- [41] This is the form of the residual environment Hamiltonian in the unmapped frame.
- [42] Maria Popovic, Mark T Mitchison, Aidan Strathearn, Brendon W Lovett, John Goold, and Paul R Eastham. Quantum heat statistics with time-evolving matrix product operators. *PRX Quantum*, 2(2):020338, 2021.
- [43] In the independent boson model that we test, the environment cannot excite the system due to the system and interaction Hamiltonians commuting.
- [44] Martí Perarnau-Llobet, Karen V Hovhannisyian, Marcus Huber, Paul Skrzypczyk, Nicolas Brunner, and Antonio Acín. Extractable work from correlations. *Physical Review X*, 5(4):041011, 2015.
- [45] Akira Sone and Sebastian Deffner. Quantum and classical ergotropy from relative entropies. *Entropy*, 23(9):1107, 2021.
- [46] Barış Çakmak. Ergotropy from coherences in an open quantum system. *Physical Review E*, 102(4):042111, 2020.
- [47] Akram Touil, Barış Çakmak, and Sebastian Deffner. Ergotropy from quantum and classical correlations. *Journal of Physics A: Mathematical and Theoretical*, 55(2):025301, 2021.
- [48] Alessandra Colla and Heinz-Peter Breuer. Thermodynamic roles of quantum environments: From heat baths to work reservoirs. *arXiv preprint arXiv:2408.00649*, 2024.